

文章编号:1001-9014(2007)04-0241-05

NOVEL COMPOSITE-CHANNEL $\text{Al}_{0.3}\text{Ga}_{0.7}\text{N}/\text{Al}_{0.05}\text{Ga}_{0.95}\text{N}/\text{GaN}$ HEMT MMIC VCO WITH LOW PHASE NOISE

CHENG Zhi-Qun¹, CAI Yong², LIU Jie², ZHOU Yu-Gang², LIU Zhi-Mei², CHEN Jing²

(1. Microelectronics CAD Center, Hangzhou Dianzi University, Hangzhou 310018, China;

2. Dept. of ECE, Hong Kong University of Science and Technology, Hong Kong, China)

Abstract: A novel structure composite-channel $\text{Al}_{0.3}\text{Ga}_{0.7}\text{N}/\text{Al}_{0.05}\text{Ga}_{0.95}\text{N}/\text{GaN}$ HEMT (CC-HEMT) microwave monolithic integrated circuit voltage-controlled oscillator (VCO) was designed, fabricated and characterized. The CC-HEMT has $1\mu\text{m} \times 100\mu\text{m}$ gate. The inter-digitated metal-semiconductor-metal (MSM) varactor is used to tune the frequency of VCO. The polyimide dielectric layer is inserted between the major metal traces and GaN buffer to improve Q factor of spiral inductors. The VCO exhibits frequency range between 7.04 ~ 7.29GHz with varactor voltage from 5.5V to 8.5V and average output power of 10dBm and average efficiency of 10.4% at bias gate of -3V and bias drain of 6V. The measured phase noise is -86.25dBc/Hz and -108dBc/Hz at offset frequency of 100 kHz and 1 MHz at varactor voltage (V_{tune}) of 6.7V. This is almost average phase noise in the range of tuning frequency. To our knowledge, this is the best reported phase noise for GaN monolithic GaN HEMT VCO.

Key words: $\text{Al}_{0.3}\text{Ga}_{0.7}\text{N}/\text{Al}_{0.05}\text{Ga}_{0.95}\text{N}/\text{GaN}$ HEMT; microwave monolithic integrated circuit (MMIC); voltage-controlled oscillator (VCO); phase noise

CLC number: TN713 Document: A

新型复合沟道 $\text{Al}_{0.3}\text{Ga}_{0.7}\text{N}/\text{Al}_{0.05}\text{Ga}_{0.95}\text{N}/\text{GaN}$ HEMT 低相位噪声微波单片集成压控振荡器

程知群¹, 蔡勇², 刘杰², 周玉刚², 刘稚美², 陈敬²

(1. 杭州电子科技大学 微电子 CAD 研究所, 浙江 杭州 310018; 2. 香港科技大学 电子与计算机工程系, 香港)

摘要: 设计并研制了一种新型复合沟道 $\text{Al}_{0.3}\text{Ga}_{0.7}\text{N}/\text{Al}_{0.05}\text{Ga}_{0.95}\text{N}/\text{GaN}$ HEMT (CC-HEMT) 微波单片集成压控振荡器 (VCO), 且测试了电路的性能。CC-HEMT 的栅长为 $1\mu\text{m}$, 栅宽为 $100\mu\text{m}$ 。叉指金属-半导体-金属 (MSM) 变容二极管被设计用于调谐 VCO 频率。为提高螺旋电感的 Q 值, 聚酰亚胺介质被插入在电感金属层与外延在蓝宝石上 GaN 层之间。当 CC-HEMT 的直流偏置为 $V_g = -3\text{V}$, $V_{ds} = 6\text{V}$, 变容二极管的调谐电压从 5.5V 到 8.5V 时, VCO 的频率变化从 7.04GHz 到 7.29GHz, 平均输出功率为 10dBm, 平均功率附加效率为 10.4%。当加在变容二极管上电压为 6.7V 时, 测得的相位噪声为 -86.25dBc/Hz (在频偏 100kHz 时) 和 -108dBc/Hz (在频偏 1MHz 时), 这个结果也是整个调谐范围的平均值。据我们所知, 这个相位噪声测试结果是文献报道中基于 GaN HEMT 单片 VCO 的最好结果。

关键词: $\text{Al}_{0.3}\text{Ga}_{0.7}\text{N}/\text{Al}_{0.05}\text{Ga}_{0.95}\text{N}/\text{GaN}$ 高电子迁移率晶体管; 微波单片集成电路; 压控振荡器; 相位噪声

Introduction

The requirement of low phase noise in VCO has

been driven by the applications of communication, the radar and high rapid data transfer. In addition, cost concerns require that the chip area should be as small

Received date: 2006-12-05, revised date: 2007-03-27

收稿日期: 2006-12-05, 修回日期: 2007-03-27

Foundation item: National Science Foundation of China (60476035)

Biography: CHENG Zhi-Qun (1964-), male, Chaohu, China, Prof. Research area is MMIC and transceiver module design.

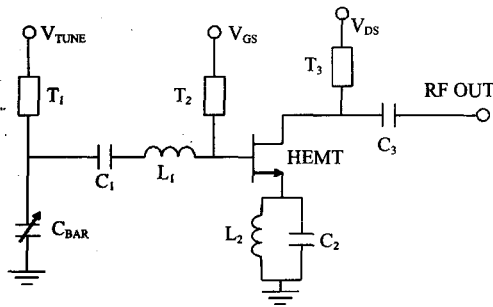


Fig. 1 Schematic of GaN MMIC VCO
图1 GaN MMIC VCO 示意图

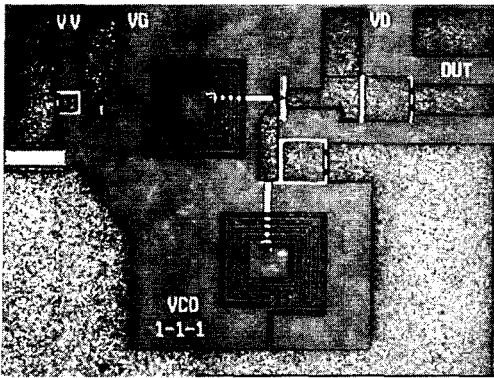


Fig. 2 Fabrication picture of GaN MMIC VCO
图2 GaN MMIC VCO 实物照片

as possible. In order to achieve smaller chip area and improve the reliability of circuits. Microwave monolithic integrated circuits are developed rapidly. Current MMIC VCOs mainly use GaAs-based, InP-based and SiGe-based high electron mobility transistors (HEMTs)^[1]. Recently, AlGaIn/GaN HEMTs show excellent microwave power performance^[2-4] and microwave noise performance^[5-12]. The high power and low phase noise oscillators have been reported^[13-17]. Monolithic GaN HEMT VCO was only reported by Valery S. Kaper et al.^[17]. This work reports a monolithic integrated VCO with novel structure $\text{Al}_{0.3}\text{Ga}_{0.7}\text{N}/\text{Al}_{0.05}\text{Ga}_{0.95}\text{N}/\text{GaN}$ HEMT employed in a $1\mu\text{m}$ -gate-length technology. The phase noise of the VCO is improved with a comparison as paper^[17]. The VCO demonstrates low phase noise of $-86.25\text{dBc}/\text{Hz}$ and $-108\text{Bc}/\text{Hz}$ at offsets of 100 kHz and 1 MHz. It is the best result for reported monolithic GaN HEMT VCO's.

1 Circuit design and simulation

The circuit was simulated by using Agilent ad-

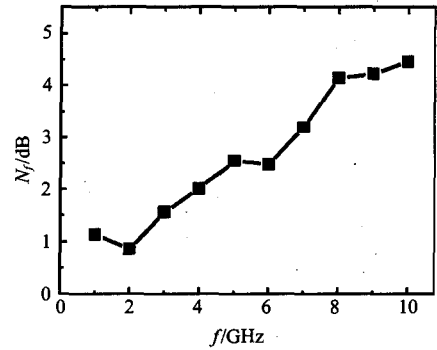


Fig. 3 Minimum noise figure N_f vs. frequency f for GaN HEMT

图3 GaN HEMT 最小噪声系数 N_f 随频率 f 变化

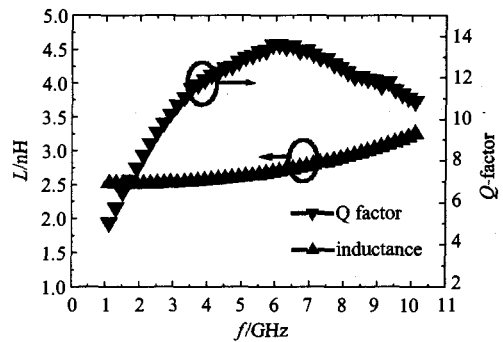


Fig. 4 High frequency characteristics of on-chip spiral inductor. L is inductance.

图4 在片螺旋电感 L 的高频特性

vanced design system (ADS) software. The schematic circuit and the fabrication picture of VCO are showed in Fig. 1 and Fig. 2 respectively. The VCO occupies an area of $1.2 \times 1.05\text{mm}^2$. As we know, low noise active device and high Q inductors and varactors are important factors to achieve low phase noise VCO. A novel structure $\text{Al}_{0.3}\text{Ga}_{0.7}\text{N}/\text{Al}_{0.05}\text{Ga}_{0.95}\text{N}/\text{GaN}$ HEMT was designed as active device of VCO in our design. The epitaxial layer structure grown by MOCVD on (0001) sapphire substrate is different from the conventional AlGaIn/GaN HEMT, a thin layer (6nm) of AlGaIn with 5% Al composition was incorporated between the $\text{Al}_{0.3}\text{Ga}_{0.7}\text{N}$ barrier and the GaN buffer, aiming at reducing the alloy scattering at the barrier interface. This novel structure $\text{Al}_{0.3}\text{Ga}_{0.7}\text{N}/\text{Al}_{0.05}\text{Ga}_{0.95}\text{N}/\text{GaN}$ HEMT exhibits excellent noise figure which is less than 3dB at frequency of C-band, as shown in fig. 3. A maximum drain current density of $910\text{mA}/\text{mm}$ and DC extrinsic transconductance (G_m) of $175\text{ms}/\text{mm}$ were obtained.

The details for its DC performances can be found in^[5]. In the design of inductor, a polyimide dielectric layer ($5\mu\text{m}$ thick) was inserted between major metal traces (transmission lines and inductor metal) and the buffer GaN grown on sapphire substrate. A maximum Q -factor of 14 was achieved at frequency of C-band. Self-resonance frequency of the inductor is over 20GHz , as shown in Fig. 4. The MSM planar inter-digitated varactors^[18], which showed improved Q -factor compared to conventional metal-insulator-semiconductor varactors, were also fabricated on the HEMT structure. A small signal S parameter of common-source GaN HEMT was used in the design of VCO. The lossless components are usually considered to form the positive feedback for the most instable HEMT. When microstrip transmission line was used to connect the source of HEMT and the ground, simulated result showed that a long microstrip transmission line was required to push HEMT into the most instable. It is bad to get small chips. When an inductor was considered instead of microstrip transmission line, simulated result showed that an inductor did not satisfy the requirement of oscillator with positive feedback. When a capacitor was considered instead of microstrip transmission line, simulated result showed that a capacitor could form positive feedback to satisfy requirement of oscillator. In order to provide direct current access, an inductor (L_2) was paralleled with feedback capacitor (C_2). After simulation, a spiral inductor ($L_2 = 4.3\text{nH}$) and MIM capacitor ($C_2 = 2.5\text{pF}$) were selected to be connected between the HEMT source and the ground. Next, a resonator circuit was designed and connected to the gate of GaN HEMT. The resonator circuit includes the spiral inductor ($L_1 = 4\text{nH}$), MIM capacitor ($C_1 = 1\text{pF}$), transmission line (T_1 and T_2), and interdigitated MSM varactor (C_{VAR}). The MIM capacitor C_1 was to decouple the bias gate voltage of HEMT's and the varactor tuning control voltage. By designing proper value of passive components of resonator, large negative resistance that is necessary for oscillation was emerging on drain port of HEMT. Then output matching network connected between drain port of GaN HEMT and 50Ω load was designed according to the oscillation conditions as follows:

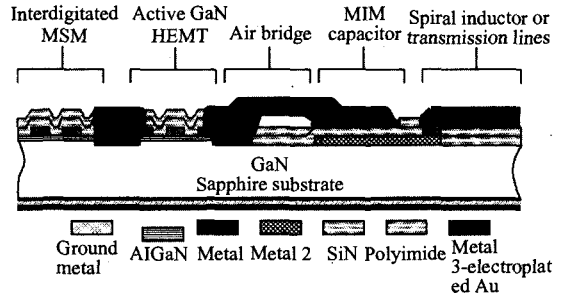


Fig. 5 Cross section of GaN-based HEMT MMIC process
图5 GaN基HEMT MMIC工艺的剖面图

$$X_L(f_0) = -\text{imag}(Z_{\text{out}}(f_0)) \quad (1)$$

$$R_L(f_0) = \frac{1}{3} |\text{real}(Z_{\text{out}}(f_0))| \quad (2)$$

where $\text{real}(Z_{\text{out}}(f_0))$ is the real part of negative resistance at the output of HEMT and $\text{imag}(Z_{\text{out}}(f_0))$ is the imaginary part of that at resonance. $R_L(f_0)$ and $X_L(f_0)$ are the real and imaginary part of the impedance looking into the load network with 50Ω load. f_0 is the resonance frequency.

2 Circuit fabrication

The sample used in this paper was grown by metal-organic chemical vapor deposition (MOCVD) on (0001) sapphire substrate. The epitaxial layer structure contains a $2.5\mu\text{m}$ undoped GaN buffer layer, a 6nm undoped $\text{Al}_{0.05}\text{Ga}_{0.95}\text{N}$ layer. The barrier layer consists of a 3nm undoped spacer, a 21nm doped ($2 \times 10^{18} \text{cm}^{-3}$) carrier supplier layer, and a 2nm undoped cap layer.

The fabrication steps of the integrated circuit include mesa isolation, source/drain ohmic contacts and gate contact formations, silicon nitride deposition and etching, polyimide gelatinization and developing, air-bridge and electroplating. The fabrication of passive components was incorporated, including microstrip transmission line, MIM capacitors, inter-digitated MSM varactors and spiral inductors. Fig. 5 shows cross section of the GaN-based HEMT MMIC process.

3 Measured results

Measurements were performed on PCB with SMA connector for RF output and off-chip bias lines for the drains, gates and varactor tuning. VCOs chips were mounted on ground metal of PCB by silver paste and its

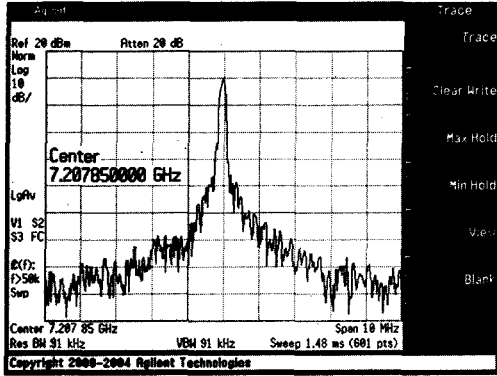


Fig. 6 Measured output spectrum at $V_{ds} = 6V$, $V_{gs} = -3V$ and $V_{tune} = 6.7V$
 图6 测试的输出频谱, 偏置电压为 $V_{ds} = 6V$, $V_{gs} = -3V$ and $V_{tune} = 6.7V$

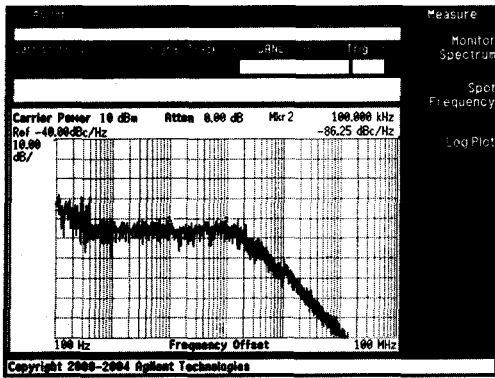


Fig. 7 Measured phase noise at offset frequency from 100Hz to 10MHz at a bias of $V_{ds} = 6V$, $V_{gs} = -3V$ and $V_{tune} = 6.7V$
 图7 在频偏从100Hz到10MHz时测试的相位噪声, 偏置电压为 $V_{ds} = 6V$, $V_{gs} = -3V$ and $V_{tune} = 6.7V$

RF output and DC bias were connected to PCB with gold wire by West Bond machine. The power and phase noise of VCO were measured by using an Agilent E4440A spectrum analyzer. Fig. 6 and Fig. 7 are output spectrum and phase noise of VCO at center frequency of 7.207GHz. The data was taken with the analyzer set to 10MHz span and a resolution bandwidth of 91kHz. The circuit is biased at $V_{gs} = -3V$, $V_{ds} = 6V$ and tuning voltage of varactor is 6.7V. The DC biases are experimentally found to be optimal for both phase noise and the tuning frequency range. The phase noise is around -86.25dBc/Hz and 108dBc/Hz at the offset frequency of 100 kHz and 1MHz respectively. At above gate and drain bias, VCO exhibits 250MHz bandwidth with center frequency of 7.136GHz, the phase noise fluctuation is 17.8 dB and 11dB at offset

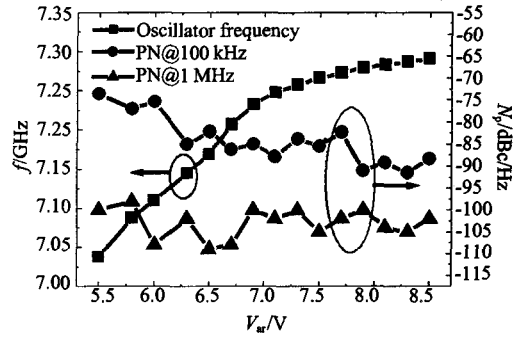


Fig. 8 The oscillator frequency f and phase noise N_p versus varactor tuning voltage V_{ar} , at a bias of $V_{ds} = 6V$, $V_{gs} = -3V$
 图8 振荡频率 f 和相位噪声 N_p 随调谐电压 V_{ar} 的变化曲线, 偏置电压为 $V_{ds} = 6V$, $V_{gs} = -3V$

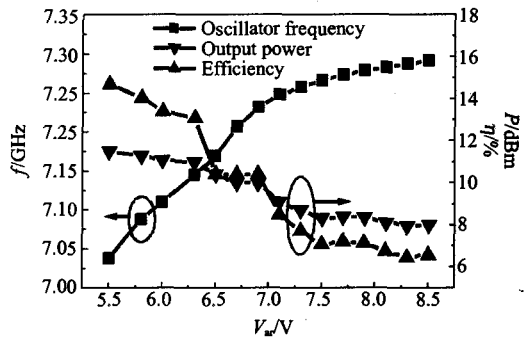


Fig. 9 Oscillator frequency f , output power P and efficiency η versus varactor tuning voltage V_{ar} , at a bias of $V_{ds} = 6V$, $V_{gs} = -3V$
 图9 振荡频率 f , 输出功率 P 和效率 η 随变容管电压 V_{ar} 的变化曲线, 偏置电压 $V_{ds} = 6V$, $V_{gs} = -3V$

frequency of 100kHz and 1MHz respectively, while tuning voltage (V_{tune}) of varactor changes from 5.5V to 8.5V as shown in Fig. 8. The efficiency changes from 14.7% to 6.5% and power changes from 11.5dBm to 7.9dBm with tuning frequencies as shown in Fig. 9.

4 Conclusion

A monolithic integrated C-band GaN VCO was designed, fabricated and characterized. The phase noise of VCO is improved by using novel structure $\text{Al}_{0.3}\text{Ga}_{0.7}\text{N}/\text{Al}_{0.05}\text{Ga}_{0.95}\text{N}/\text{GaN}$ HEMT with low noise figure and high Q spiral inductors and inter-digitated MSM varactor. The VCO exhibits phase noise of -86.25dBc/Hz and -108dBc/Hz at offsets of 100kHz and 1MHz. The phase noise is the best reported results of MMIC GaN HEMT VCO's.

REFERENCES

- [1] CHEN Ji-Xin, HONG Wei, YIN Xiao-Xing, *et al.* Development of millimeter wave VCO MMIC with low phase noise [J]. *J. Infrared Millim. Waves* (陈继新, 洪伟, 殷晓星, 等. 低相位噪声毫米波单片压控振荡器的研制. 红外与毫米波学报), 2006, **25**(4): 271—274.
- [2] Lee J W, Eastman L F, Webb K J. A Gallium-nitride push-pull microwave power amplifier [J]. *IEEE Transactions on Microwave Theory and Techniques*, 2003, **51**(11): 2243—2249.
- [3] Chung Y, Hang C Y, Cai S, *et al.* Effects of output harmonic termination on PAE and output power of AlGaIn/GaN HEMT power amplifier [J]. *IEEE Microwave and Wireless Components Lett.*, 2002, **12**(11): 421—423.
- [4] Liu J, Zhou Y G, Chu R M, *et al.* $\text{Al}_{0.3}\text{Ga}_{0.7}\text{N}/\text{Al}_{0.05}\text{Ga}_{0.95}\text{N}/\text{GaN}$ composite-channel HEMTs with enhanced linearity [J]. *IEDM Tech. Dig.*, 2004, **12**: 811—814.
- [5] Cheng Z Q, Liu J, Zhou Y G, *et al.* Broadband microwave noise characteristics of high-linearity composite-channel $\text{Al}_{0.3}\text{Ga}_{0.7}\text{N}/\text{Al}_{0.05}\text{Ga}_{0.95}\text{N}/\text{GaN}$ HEMTs [J]. *IEEE Electron Device Letters*, 2005, **26**(8): 521—523.
- [6] Lee J W, Kuliev A, Kumar V, *et al.* Microwave noise characteristics of AlGaIn/GaN HEMTs on SiC substrates for broad-band low-noise amplifiers [J]. *IEEE Transactions on Microwave Theory and Techniques*, 2004, **14**(6): 259—261.
- [7] Lu W, Kumar V, Piner E L, *et al.* DC, RF, and microwave noise performance of AlGaIn-GaN field effect transistors dependence of aluminum concentration [J]. *IEEE Trans. Electron Devices*, 2003, **50**(4): 1069—1074.
- [8] Xu H T, Sanabria C, Chini A, *et al.* A C-band high-dynamic range GaN HEMT low-noise amplifier [J]. *IEEE Microwave and Wireless Components Lett.*, 2004, **14**(6): 262—264.
- [9] Ellis G A, Moon J S, Wong D, *et al.* Wideband AlGaIn/GaN HEMT MMIC low noise amplifier [C]. Texas USA; IEEE International Microwave Symposium Digest, 2004, 153—156.
- [10] Welch R, Kumar V, Neidhard B, *et al.* Low noise hybrid amplifier using AlGaIn/GaN power HEMT devices [C]. Texas USA; Baltimore Md IEEE GaAs IC Symposium Digest, 2001, 153—155.
- [11] Cha S, Chung Y H, Wojtowicz M, *et al.* Wideband AlGaIn/GaN HEMT low noise amplifier for highly survivable receiver electronics [C]. Texas USA; IEEE International Microwave Symposium Digest, 2004, 829—832.
- [12] Schwindt R, Kumar V, Aktas O, *et al.* AlGaIn/GaN HEMT-based fully monolithic X-band low noise amplifier [J]. *Phys. Stat. Sol. (c)*, 2005, **2**(7): 2631—2634.
- [13] Xu H T, Sanabria C, Nadia K. *et al.* Low phase-noise 5GHz AlGaIn/GaN HEMT oscillator integrated with $\text{Ba}_x\text{Sr}_{1-x}\text{TiO}_3$ thin films [C]. Texas USA; IEEE MTT-S Dig., 2004, 1509—1512.
- [14] Sanabria C, Xu H T, Heikman S, *et al.* A GaN differential oscillator with improved harmonic performance [J]. *IEEE Microwave and Wireless Components Letters*, 2005, **15**(7): 463—465.
- [15] Kaper V S, Tilak V, Kim H, *et al.* High-power monolithic AlGaIn/GaN HEMT oscillator [J]. *IEEE Journal of Solid-state Circuits*, 2003, **38**(9): 1457—1461.
- [16] Shealy J B, Smart J A, Shealy J R. low-phase noise AlGaIn/GaN FET-based voltage controlled oscillators (VCOs) [J]. *IEEE Microwave and Wireless Components Letters*. 2001, **11**(6): 244—245.
- [17] Kaper V S, Thompson R M, Prunty T R, *et al.* Signal generation, control, and frequency conversion AlGaIn/GaN HEMT MMICs [J]. *IEEE Transactions on Microwave Theory and Techniques*, 2005, **53**(1): 55—65.
- [18] Chu C S, Zhou Y G, Chen K J, *et al.* Q-factor characterization of radio-frequency GaN-based metal-semiconductor-metal planar interdigitated varactors [J]. *IEEE Electron Device Letters*, 2005, **26**(7): 432—434.